RF study of a C-band barrel open cavity pulse compressor

SHU Guan(束冠)[1,2] ZHAO Feng-Li(赵风利)[1] HE Xiang(贺祥)[1]

[1] Laboratory of Particle Acceleration Physics & Technology, Institute of High Energy Physics, Chinese Academy of Sciences, Beijing 100049, China
[2] University of Chinese Academy of Science, Beijing 100049, China

Abstract: This paper focuses on the RF study of a C-band barrel open cavity (BOC) pulse compressor. The operating principle of BOC is presented and the technical specifications are determined. The main parts of BOC such as the cavity, the matching waveguide, the coupling slots and the tuning rings were numerically simulated by 3-D codes software HFSS and CST Microwave Studio (MWS). The "whispering gallery" mode $TM_{6,1,1}$ with an unload Q of 100000 was chosen to oscillate in the cavity. An energy multiplication factor of 1.99 and a peak power gain of 6.34 was achieved theoretically.

Key words: C-band, BOC pulse compressor, HFSS, MWS, energy multiplication factor, peak power gain

PACS: 41.20.-q, 07.57.-c **DOI:** 10.1088/1674-1137/39/5/057005

1 Introduction

The pulse compressor is one of the key devices of linear accelerators. At the moment, there are only SLAC energy doubler (SLED) type and barrel open cavity (BOC) type pulse compressors at C-band [1–4]. The conventional SLED is based upon two high Q resonant cavities which are connected by a 3 dB hybrid coupler to minimize the reflection [5]. Contrary to the SLED, the BOC pulse compressor consists of a single barrel open cavity and a matching waveguide. A special property of the open cavity is the resonant mode called whispering gallery mode, which has an extremely high unload Q. So the BOC is more simple, compact and economical compared to the SLED.

The study of the BOC was started for the first time at IHEP, Beijing, and a prototype made of oxygen free high conductivity copper is on the schedule, which is focused on the research of RF characterization and the mechanical brazing process.

The performance of a BOC depends on the following three characteristic values: the resonant frequency, the unload Q and the coupling coefficient. HFSS [6] was used to evaluate these parameters and the results were compared with the Microwave Studio (MWS) [7] results for verification.

2 BOC theory and choice of parameters

The BOC is composed of a barrel-shaped open cavity, a certain number of coupling slots and a waveguide wrapped around the perimeter of the cavity. Fig. 1 shows the schematic layout.

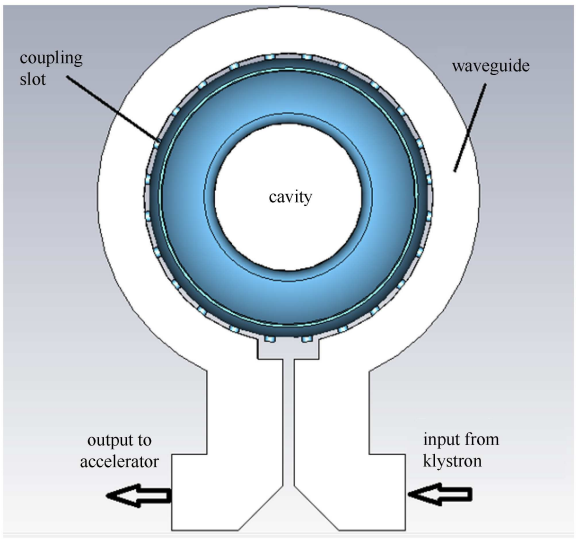

Fig. 1. (color online) The schematic layout of BOC.

The RF power is magnetically coupled from the waveguide to the cavity through dozens of coupling slots, and a fraction of it propagates around the cavity as a traveling wave. The traveling wave is synchronous with the waveguide. The adjacent coupling slots are spaced $\lambda_g/4$ apart from each other while each slot radiates a forward wave to the accelerator as well as a backward wave to the klystron. All the forward waves are in phase at BOC output and add up, while the backward waves experience a cancellation, so very little power goes back

Received 15 July 2014

to the klystron [8]. The output of the BOC is the superposition of the input wave and the emitted wave from the cavity with a phase reversal. The stored energy can be released during a much shorter period if the incoming RF pulse phase is reversed 180° in one compressed pulse time, so the peak power of the output is then enhanced at the expense of the pulse width.

According to the principle of energy conservation [5], it can be given that

$$T_{\rm c}\frac{{\rm d}E_{\rm e}}{{\rm d}t}+E_{\rm e}=-\alpha E_{\rm in}, \tag{1}$$

where $E_{\rm e}$ is the emitted wave from the cavity, $E_{\rm in}$ is the incident wave from the klystron, $\alpha=2\beta/(1+\beta)$ with β the coupling factor and $T_{\rm c}=2Q_{\rm L}/\omega_0$ is the filling time of the cavity.

Assume that the incoming RF pulse phase is reversed 180° at time t_1, and the incident power is turned off at time t_2. By solving Eq. (1), the output wave to the accelerator structures can be given as:

$$\begin{aligned} E_{\rm L}(A) &= (\alpha-1)-\alpha{\rm e}^{-\tau} \quad 0\leqslant t<t_1 \\ E_{\rm L}(B) &= \gamma{\rm e}^{-(\tau-\tau_1)}-(\alpha-1) \quad t_1\leqslant t<t_2 \\ E_{\rm L}(C) &= [\gamma{\rm e}^{-(\tau_2-\tau_1)}-\alpha]{\rm e}^{-(\tau-\tau_2)} \quad t_2\leqslant t \end{aligned} \tag{2}$$

where $\tau=t/T_{\rm c}$, $\gamma=\alpha(2-{\rm e}^{-\tau_1})$. The relationship between $E_{\rm in}$, and $E_{\rm L}$ is shown in Fig. 2.

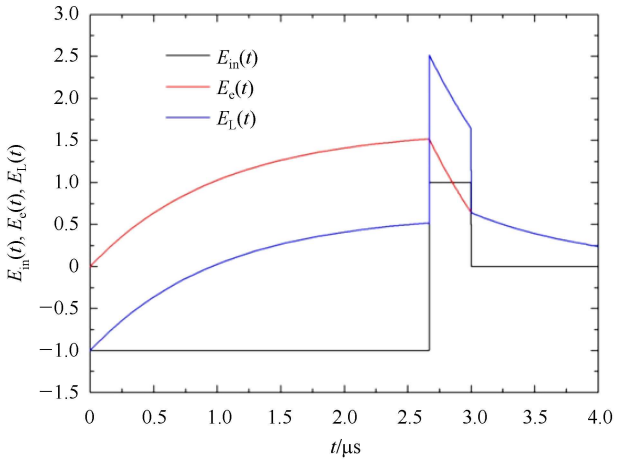

Fig. 2. (color online) Amplitudes of the input wave $E_{\rm in}$, emitted wave $E_{\rm e}$ and the output wave $E_{\rm L}$.

Considering the performance and fabrication cost of the prototype, the $\rm TM_{6,1,1}$ mode with an unload Q factor of 100000 was finally chosen as the resonant mode. Fig. 3 shows the relationship between the energy multiplication factor and the coupling coefficient while the pulse length is set as 3 μs and the phase is reversed at 2.67 μs.

A maximum energy multiplication factor of 1.99 (when the coupling coefficient β=4.5) is allowed by the specifications of the accelerator and the input pulse. The main technical parameters of the designed BOC are listed in Table 1.

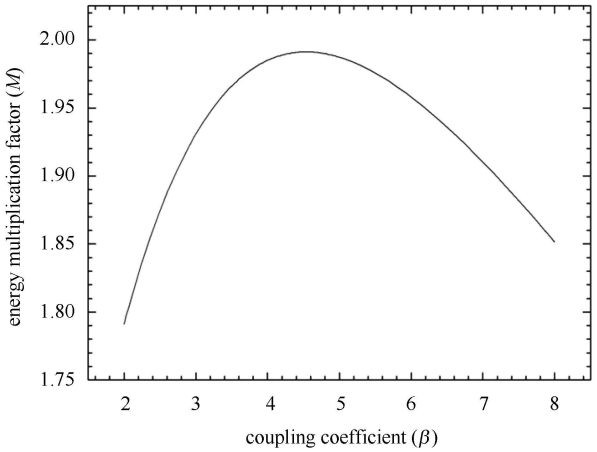

Fig. 3. Relationship between the energy multiplication factor and the coupling coefficient.

Table 1. Technical specifications of the BOC pulse compressor.

pulse compressor	design parameter
resonant frequency/MHz	5712
resonant mode	$\rm TM_{6,1,1}$
unload Q	∼100000
coupling coefficient(β)	4.5
RF input pulse length/μs	3.0
RF compressed pulse length/μs	0.33
energy multiplication factor(M)	1.99
peak power gain	6.34
effective power gain	4.29

3 RF design and simulations

3.1 Resonant cavity

The characteristics of the open cavity are decided by its internal geometric dimensions. The target mode is activated in the cavity after being reflected by the cavity internal surface repeatedly, while other parasitic modes radiate away through the two open ports. The spectrum of the cavity is quite sparse.

Figure 4 shows the profile of the barrel shape cavity. The resonant frequencies of the barrel cavity operating in $\rm TM_{mnq}$ modes have been given by [8–11]

$$ka=\nu_{\rm mn}+\frac{(q-1/2)\alpha}{\sin\theta}, \tag{3}$$

where k is the wavenumber in free space, a is the radius of the cavity median plane, $v_{\rm mn}$ is the nth root of the mth order of Bessel function. α and θ can be derived from

$$\sin\alpha = \sqrt{\frac{a}{r_0}}\sin\theta, \tag{4}$$

$$\cos\theta = \frac{m}{\nu_{\rm mn}}, \tag{5}$$

where r_0 is the cavity wall radius.

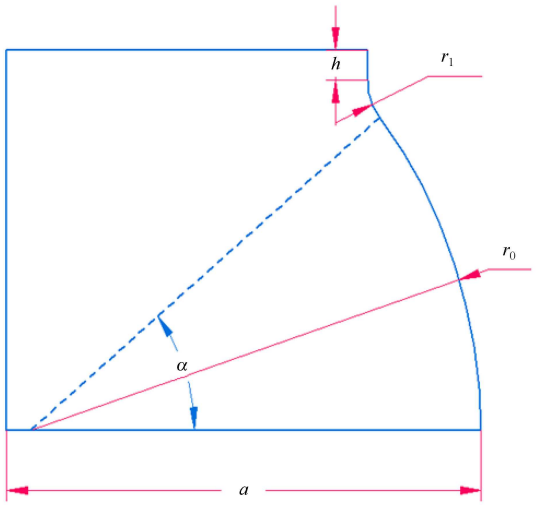

Fig. 4. (color online) Barrel cavity profile.

The unload Q can be written simply as

$$Q=\frac{a}{\delta}, \tag{6}$$

where δ is the skin depth. At 5.712 GHz, the skin depth of copper is about 0.874 μm. The "whispering gallery" mode is chosen in BOC, and in order to obtain a high Q value, the surface flatness should be much smaller than the skin depth.

Compared to the target value of 5712 MHz, the cavity was first designed to resonate at a higher frequency (set as 5713 MHz) to leave some room for frequency adjustment. Table 2 shows the theoretical and calculated value of the BOC cavity. Comparison of the HFSS and CST results with the theoretical ones demonstrates excellent agreement.

Table 2. Theoretical and calculated value of the BOC cavity.

parameter	theoretical	HFSS	CST
frequency/MHz	5713.00	5713.97	5713.94
unload Q	100600	100300	100300

Figure 5 shows the electric energy density distribution of the $TM_{6,1,1}$ mode. The power is concentrated near the curved surface.

3.2 Coupling between the cavity and the waveguide

As mentioned in Section 2, in order to protect the RF source, the distance of adjacent slots is chosen as $\lambda_g/4$ to reduce the backward wave to the klystron. 24 identical coupling slots are located between the cavity and the waveguide due to the resonant mode $TM_{6,1,1}$ in the cavity. Phase velocities in the waveguide and cavity are matched by adjusting the width of the waveguide.

The theoretical width of the waveguide is given by [12]:

$$\frac{2\pi(a+\Delta+w)}{6}=\frac{\lambda_0}{\sqrt{1-(\lambda_0/2w)^2}}, \tag{7}$$

where w is the width of the waveguide, a is the radius of the cavity median plane, Δ is the thickness of a slot, λ_0 is the wavelength of resonant frequency in free space.

The dimensions of the waveguide were optimized by HFSS and then the whole model simulation was carried out. The electric field distribution of the median plane of the BOC is presented in Fig. 6.

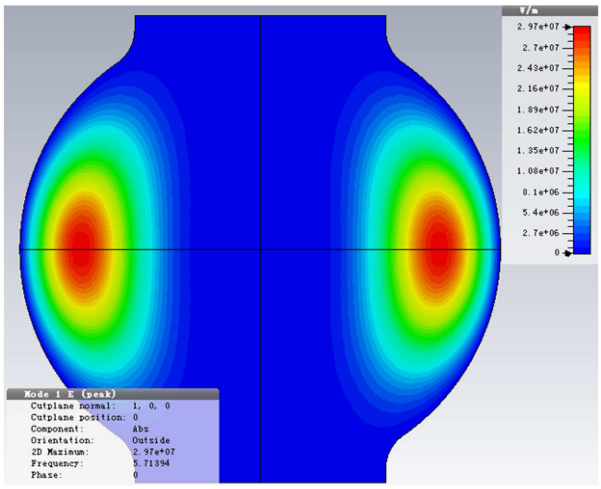

Fig. 5. (color online) $TM_{6,1,1}$ mode electric energy density distribution on cut planes simulated by CST.

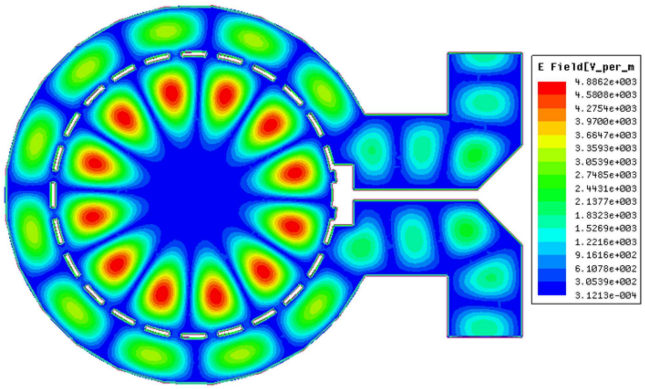

Fig. 6. (color online) Electric field distribution on a median plane of BOC pulse compressor simulated by HFSS.

The coupling coefficient is determined by the size of the slots. The relationship between the coupling coefficient and the radius of the coupling slots is illustrated in Fig. 7. For the prototype, the radius is chosen as 3.0 mm at first and then enlarged gradually during measurement.

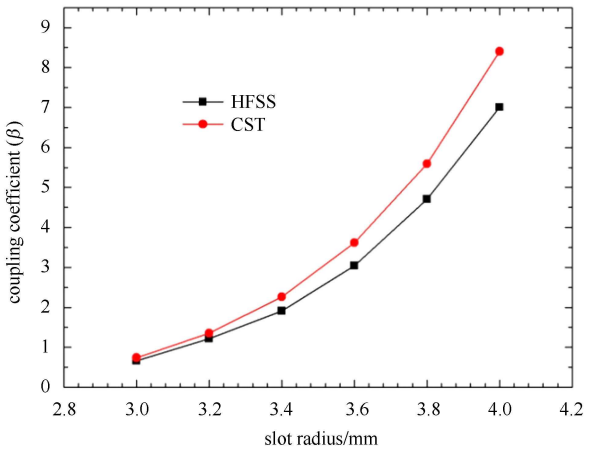

Fig. 7. (color online) Dependence of the coupling coefficient on the diameter of the slot.

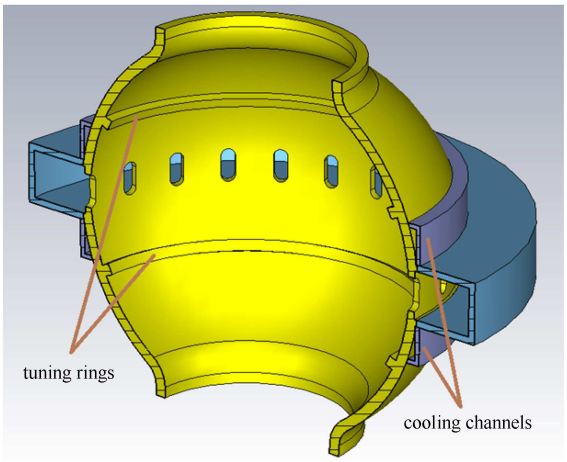

Fig. 8. (color online) Positions of the tuning components.

3.3 Tuning

Two tuning rings are bulged symmetrically to the median plane in the internal surface of the cavity (Fig. 8 shows the tuning component positions). The resonant frequency decreases by cutting the rings. Then, the final tuning of the frequency is realized by controlling the temperature of the water in the water cooling system during the BOC operation. Coarse tuning of the frequency is realized by mechanical cutting, and temperature control system is used for fine tuning [2].

Figure 9 shows the relationship between the resonant frequency (unload Q) of the cavity and the tuning ring radius. The dimensions of the tuning ring were optimized for achieving an adequate tuning range while not affecting the Q-factor of the operating $TM_{6,1,1}$ mode too much. The tuning sensitivity was about 4.4 MHz/mm.

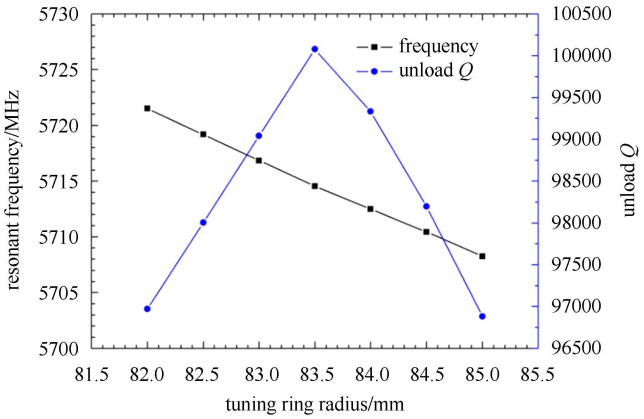

Fig. 9. (color online) Relationship between the frequency (unload Q) and the tuning ring radius simulated by HFSS.

4 Conclusions

The design of a C-band BOC pulse compressor with the help of HFSS and MWS software is presented in this paper. The BOC prototype is aimed at the research of the RF characterizations with low power, and to check the reliability of the simulations. The study of the high power RF electromagnetic effect on the BOC will be carried out later. The cooling channels and the fine tuning systems will be designed according to the RF-thermal-structural-RF coupled analysis.

References

1 Sugimura T, Kamitani T, Yokoyama K et al. SKIP-A Pulse Compressor for Superkekb. Proc. of LINAC 2004, 2004. 754–756
2 Zennaro R, Bopp M, Citterio A et al. C-BAND RF Pulse Compressor for Swissfel. Proc. of IPAC13, 2013. 2827–2829
3 XIAO Ou-Zheng, ZHAO Feng-Li, HE Xiang. CPC (HEP &NP), 2012, **36**(4): 376–379
4 XIAO Ou-Zheng, ZHAO Feng-Li. CPC (HEP & NP), 2012, **36**(11): 1132–1135
5 Farkas Z D, Hogg H A, Loew G A et al. SLED: A Method of Doubling SLAC's Energy. The 9th International Conference on High Energy Accelerators, 1974. SLAC-PUB-1453
6 HFSS User's Guide. ANSOFT Corporation
7 Microwave Studio, Computer Simulation Technology, Darmstadt, Germany. www.cst.com
8 Bossart R, Brown P, Mourier J et al. High-Power Microwave Pulse Compression of Klystrons by Phase-Modulation of High-Q Storage Cavities. CERN-OPEN-2004-015
9 Syrachev I V. The Progress of X-Band "Open" Cavity RF Pulse Compression Systems. Proc. of EPAC94, 1994. 375–379
10 Brown P, Syratchev I. 3 GHz Barrel Open Cavity (BOC) RF Pulse Compressor for CTF3. Microwave Symposium Digest, 2004 IEEE MTT-S International, 2004. 1009–1012
11 Balakin V E, Syrachev I V. Status VLEPP RF Power Multiplier(VPM). Proc. of EPAC92, 1992. 1173–1175
12 Bossart R et al. CTF3 Design Report. CERN-PS-2002-008-RF